

## NUMERICAL SIMULATIONS OF THE OXYGEN IMPURITY TRANSPORT AT THE PLASMA PERIPHERY IN A TOKAMAK

M. Tendler, Royal Institute of Technology, Stockholm, Sweden;  
and

J. Neuhauser and R. Wunderlich, Max-Planck-Institut für Plasmaphysik, EURATOM Association, D-8046 Garching, Germany.

### INTRODUCTION

The behaviour of oxygen, which is one of the most frequently encountered impurity species in tokamaks, is particularly complicated due to the intensive cross charge exchange processes between oxygen and hydrogen. The other complications arise due to the fact that oxygen is desorbed from the metallic surfaces as hydrogenic or metallic compounds, undergoing a sophisticated multistep evolution before arriving at the neutral atomic state.

Here, we aim at studying the influence of these effects, using the numerical algorithm, which allows a fast solution of both the steady-state and the time-dependent one-dimensional finite rate diffusion equation /1/. The auxiliary calculations, accounting for the cross charge exchange and the sub-routine, describing the low energy chemical kinetics are incorporated in the code.

### RESULTS AND DISCUSSIONS

The cross charge exchange processes affect both oxygen neutrals and the singly ionized oxygen ions, if their mean free paths for charge exchange are of the same order as the ionization mean free path.

For oxygen atoms, injected with an initial energy much less than the plasma temperature, the cross charge exchange processes dominate over the ionization by the electron impact, producing fast oxygen neutrals with an average energy of the order of the plasma temperature and at the same time retarding their directed motion by randomizing their velocity distribution. Some part of the oxygen neutrals (roughly one half for low temperatures) returns to the wall reducing the flux of the injected impurities. The other part, moving into the plasma, penetrates much deeper due to the increased velocity reaching the region with the higher temperature, where the ionization to the second ionization state by electron impact increases drastically and the amount of the neutral hydrogen decreases.

The charge exchange processes with hydrogen affect not only the oxygen neutrals but also the diffusion of the singly ionized oxygen ions. They diffuse much faster as a result of the multiple charge exchange collisions and thus undergo greater recycling. It implies an increase of the effective diffusion coefficient of the singly ionized oxygen ions as described in /2/.

To demonstrate some of the typical examples of the 1-D multispecies, non-corona impurity transport code, some steady radial density profiles for oxygen are given in Figs. 1 and 2 for temperature and density profiles similar to those of an ohmically heated ASDEX plasma.

The effect of the cross charge exchange plays an important role if the neutral hydrogen flux exceeds the value  $10^{17} \text{ cm}^{-2} \text{ sec}^{-1}$  for the plasma tempera-

ture at the wall equal to 10 eV, scaling slower than the penetration depth of oxygen neutrals for a given flux density, due to the increased albedo of the plasma. The enhancement factor for the total impurity content is 5 - 6 for the hydrogen flux changing from  $10^{17}$  to  $10^{19}$   $\text{cm}^{-2}\text{sec}^{-1}$ . (Fig.4). Though the latter flux might appear excessive compared with the typical value averaged over the flux surfaces, due to the significant poloidal and toroidal asymmetries observed in the outer regions of the tokamak plasma, this value, corresponding to  $n_{\text{H}} \leq n_e$ , can locally become of the right order of magnitude. This is certainly true for the regions with the large content of the neutral hydrogen, such as the area in the close vicinity of the limiter's top /4/ or the gas inlet.

Significant modifications appear also in the distribution of the oxygen ions over the ionization states. The low ionization states are usually located at the periphery and therefore strongly influenced by the cross charge exchange processes. Owing to the enhanced diffusion, the amount of impurities in the low ionization states (0 II - 0 V) decreases, their profiles get flatter at the much lower level. It might be one of the reasons for the observational difficulties of these ions /3/. On the other hand, the relative amount of the higher ionization states increases, leading to the growing radiative efficiency. The other important implication of the effect occurs if the decay length is much larger than the mean free path for charge exchange. It might lead to increased oxygen recycling at the first wall instead of, as usual, taking place at the limiter. The effect gets less important with the decreasing value of the decay length in the scrape-off, owing to the rapid loss of the 0 II at the limiter. For obvious reasons the total amount of impurities gets smaller by one order of magnitude if the decay length is less than the width of the limiter and the penetration depth of the impurity neutrals. (Fig.4).

As far as molecules are concerned, the drastically increased penetration depth of the oxygen impurities is the result of the low energy chemical processes occurring to the oxygen molecular compounds, released from the wall. For the case of ASDEX it reaches the values up to 5 - 10 cm. The profile of the total number of impurity ions is shown in Fig. 3. Important consequences arise from the combination of these effects with charge exchange: the penetration depth of the atomic impurities increases further and much less (roughly one fourth) of the oxygen atoms produced from the molecular compounds return to the wall. The total number of impurities scales even stronger than the penetration depth of oxygen atoms for a given inflow of impurities.

#### ACKNOWLEDGEMENTS

The authors wish to thank Prof. B. Lehnert and Dr. K. Lackner for discussions.

#### REFERENCES

- /1/ K. Lackner et al., Z. Naturforsch. 37a, 931, 1982
- /2/ M. Tendler, Pl. Phys. July 1983
- /3/ TFR Group, Nucl. Fus. 22, 1173, 1982
- /4/ S. Allen et al., Nucl. Fus. 21, 251, 1981.

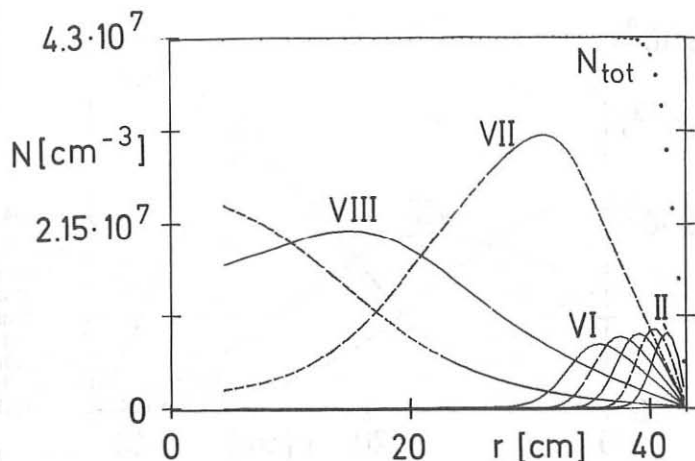


Fig. 1: Profiles of oxygen ionization states for hydrogen and oxygen fluxes  $\Gamma_{\text{H}} = 0$ , or  $\Gamma_{\text{O}} = 10^{11} \text{ cm}^{-2} \text{ sec}^{-1}$ , respectively. Dashed and solid lines are used for even and odd ionization states respectively. The dotted line gives the total density of the oxygen ions. The scrape-off layer is switched off.

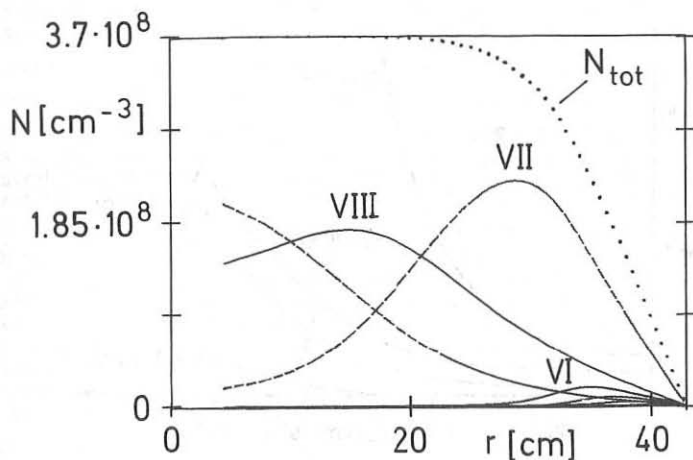


Fig. 2: Profiles of oxygen ionization states for the hydrogen flux  $\Gamma_{\text{H}} = 10^{19} \text{ cm}^{-2} \text{ sec}^{-1}$ . Otherwise, notations and conditions are the same as for Fig. 1.

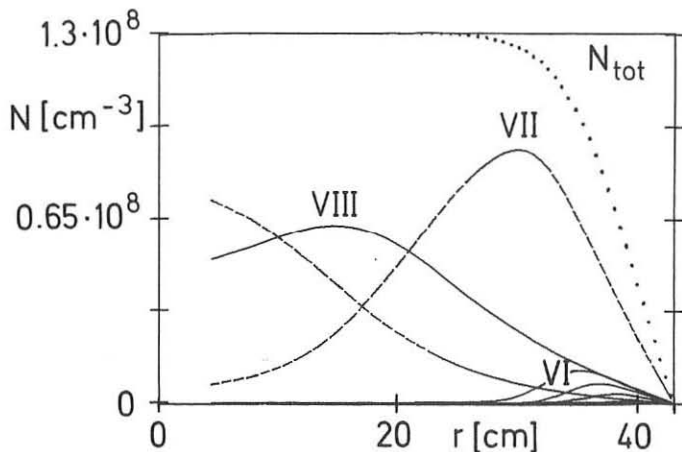


Fig. 3: Profiles of oxygen ionization states for the density of the oxygen molecules  $N_{MOL} = 10^7 \text{ cm}^{-3}$  and an energy 0.03 eV at the wall. The oxygen atomic flux  $\Gamma_o = 0$ . Otherwise, the same as for Figs. 1 and 2.

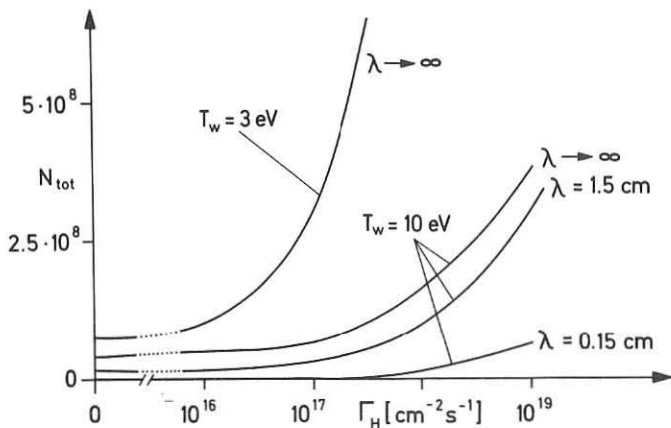


Fig. 4: Maximum total oxygen ion density as functions of hydrogen flux for different plasma decay lengths  $\lambda$  and wall temperatures  $T_w$ . For  $T_w = 10 \text{ eV}$ , the drastic increase occurs when the hydrogen flux changes from  $\Gamma_H = 10^{17}$  to  $\Gamma_H = 10^{19} \text{ cm}^{-2} \text{ sec}^{-1}$ .